

UC Irvine

UC Irvine Previously Published Works

Title

Direct 120V, 60Hz operation of an organic light emitting device

Permalink

<https://escholarship.org/uc/item/4355p9n4>

Journal

Journal of Applied Physics, 99(7)

ISSN

0021-8979

Authors

Slinker, Jason D
Rivnay, Jonathan
DeFranco, John A
[et al.](#)

Publication Date

2006-04-01

DOI

10.1063/1.2186031

Peer reviewed

Direct 120 V, 60 Hz operation of an organic light emitting device

Jason D. Slinker, Jonathan Rivnay, John A. DeFranco, Daniel A. Bernards, Alon A. Gorodetsky, Sara T. Parker, Marshall P. Cox, Richard Rohl, and George G. Malliaras^{a)}

Department of Materials Science and Engineering, Cornell University, Ithaca, New York 14853-1501

Samuel Flores-Torres and Héctor D. Abruña

Department of Chemistry and Chemical Biology, Cornell University, Ithaca, New York 14853-1301

(Received 13 October 2005; accepted 20 January 2006; published online 5 April 2006)

We report on lighting panels based on ruthenium(II) tris-bipyridine complexes that can be sourced directly from a standard US outlet. With the aid of the ionic liquid 1-butyl-3-methylimidazolium, the conductivity of the light emitting layer was enhanced to achieve device operation at a 60 Hz frequency. Lighting panels were prepared using a cascaded architecture of several electroluminescent devices. This architecture sustains high input voltages, provides fault tolerance, and facilitates the fabrication of large area solid-state lighting panels. Scalability of the drive voltage, radiant flux, and external quantum efficiency is demonstrated for panels with up to $N = 36$ devices. Direct outlet operation is achieved for panels with $N = 16, 24,$ and 36 devices. © 2006 American Institute of Physics. [DOI: 10.1063/1.2186031]

I. INTRODUCTION

Organic electroluminescent devices are being developed for solid-state lighting applications due to their ease of fabrication, compatibility with glass and plastic substrates, color purity, and potential as highly efficient emitters.^{1,2} Presently, lighting accounts for about 20% of the energy used in the United States, at an economic cost of \$12 billion and an environmental cost of over 10 million metric tons of carbon emission per year.¹ Organic electroluminescent devices have the potential to surpass the 60–100 lm/W power efficiency of commercial fluorescent lamps, and they are amenable to cost-effective fabrication such as inkjet printing and reel-to-reel processing on flexible substrates.^{1,2}

The majority of organic electroluminescent devices presently under study and development are light emitting diodes (LEDs).² A conventional LED achieves hole and electron injection with a high work function anode and a low work function cathode, respectively. An appreciable current passes through the device only upon application of a forward bias, so light emission is only visible for positive voltages. Furthermore, application of a reverse bias can often lead to electrochemical degradation of the low work function contact and failure of the device. For these reasons, conventional light emitting diodes are not directly functional with an ac voltage signal symmetric about 0 V—an ac/dc converter or dc voltage offset is necessary for compatibility. However, the most common voltages for fixed light source applications are pure ac signals, for example, as supplied by a standard household outlet. Clearly, a light emitting device that is directly compatible with ac voltage signals is desirable.

A recent concept in solid-state electroluminescent devices involves the use of ionic transition metal complexes (iTMCs).^{3–12} These devices differ significantly from conven-

tional organic light emitting diodes due to the presence of mobile ions in the organic film. A prototypical example of an iTMC is the ruthenium complex $[\text{Ru}(\text{dtb-bpy})_3]^{2+}(\text{PF}_6^-)_2$ (where dtb-bpy is 4,4'-di-*t*-butyl-2,2'-bipyridyl). An electroluminescent device is fabricated by sandwiching a thin (ca. 100 nm) film of $[\text{Ru}(\text{dtb-bpy})_3]^{2+}(\text{PF}_6^-)_2$ between two metal contacts. Upon application of a bias, and according to the electrodynamic model,^{12,13} the counter ions (PF_6^-) redistribute and create high electric fields near the contacts. Electrons and holes are subsequently injected into the metal complexes ($[\text{Ru}(\text{dtb-bpy})_3]^{2+}$), where they migrate towards each other by means of hopping and recombine within a single metal complex to produce light. Electroluminescent devices based on iTMCs offer ease of fabrication, as they consist of a single layer of organic that is deposited from solution. In addition, contrary to conventional LEDs that require low work function cathodes, they show efficient operation even with air-stable cathodes.¹⁴ This enables fabrication by means of lamination¹⁵ as well as the development of fault-tolerant architectures for large area illumination panels.¹⁶

This work demonstrates the fabrication and operation of “plug and play” organic light emitting devices that can be sourced directly from a standard US outlet, namely, 110–120 V rms and 60 Hz. This is the most readily available source voltage signal for domestic lighting applications. This work demonstrates a technique for developing large area solid-state lighting panels that are cost effective and fault tolerant, which supports the implementation of organic electroluminescent devices for general lighting purposes.

II. EXPERIMENTAL PROCEDURE

The preparation of the solutions, device fabrication, and device testing were all performed in a nitrogen glove box. The synthesis of the ionic transition metal complex $[\text{Ru}(\text{dtb-bpy})_3]^{2+}(\text{PF}_6^-)_2$, where dtb-bpy is 4,4'-di-*tert*-butyl-2,2'-bipyridyl, has been reported elsewhere.⁸ This complex

^{a)} Author to whom correspondence should be addressed; electronic mail: ggm1@cornell.edu

was chosen because a series of tests with various Ru complexes revealed that it showed the best phase compatibility with the ionic liquid used in this study. The ionic liquid 1-butyl-3-methyl-imidazolium hexafluorophosphate $\text{BMIM}^+(\text{PF}_6^-)$ was purchased from Aldrich (Fluka) and used as received. Sandwich-type devices were fabricated by dissolving the Ru complex in acetonitrile at a concentration of 24 mg/mL, and spin coating onto glass substrates covered with prepatterned indium tin oxide (ITO) contacts (Thin Film Devices, Anaheim, CA) at 1000 rpm. In the case of the high voltage cascaded panels, the ITO was patterned by conventional photolithography. For devices incorporating ionic liquid, 10 μL of $\text{BMIM}^+(\text{PF}_6^-)$ were added per mL of solution. This amount was close to the upper limit before phase separation became visible with an optical microscope. The thickness of the films was approximately 100 nm. The ITO substrates were cleaned just before the deposition of the organic layer by a de-ionized water bath, followed by UV/ozone treatment. The films were dried for 18 h under a high vacuum with a base pressure of less than 2×10^{-6} torr. The top contacts consisted of 200 Å thick Au films. This deposition was carried out intermittently to minimize heating of the organic film. In the case of single devices, the Au contacts were deposited through a shadow mask that defined six devices per substrate, each with a 3 mm² active area. The contacts for the high voltage cascaded panel were deposited through a Si wafer shadow mask defining 96 devices per substrate, each with a 1 mm² active area. This mask was patterned by photolithography and etched with a Unaxis 770 plasma etcher employing a Bosch etch technique. In the case of the cascaded lighting panel, the Au contacts were deposited through a shadow mask that defined 16 devices per substrate, each with a 9 mm² active area. These contacts were deposited on polydimethylsiloxane (PDMS) and laminated according to a method described previously.¹⁵ The electrical characteristics of the devices operating under dc conditions were measured with a Keithley 236 source-measure unit, while ac current measurements were performed with a Fluke 87 III Multimeter. The ac power was supplied by either a Hewlett-Packard wave form generator for 7 V rms operation or directly from the line and neutral leads from a standard US outlet. The radiant flux measurements were collected with a calibrated UDT S370 optometer coupled to an integrating sphere or with a fast photodiode connected to a Hewlett-Packard 54616B oscilloscope. The EL spectra were measured with a calibrated S2000 Ocean Optics fiber spectrometer.

III. RESULTS AND DISCUSSION

The current and radiant flux of a standard single ITO/ $[\text{Ru}(\text{dtb-bpy})_3]^{2+}(\text{PF}_6^-)_2/\text{Au}$ device operating under +3, -3, and 5 V dc are depicted in Fig. 1. Unlike a conventional LED, light emission is observed at the same intensity for both +3 and -3 V operations (forward and reverse bias). Stable operation for positive and negative voltages is requisite for efficient operation from ac source signals. However, about 60 s of operation are needed to achieve turn on of the device, that is, to achieve maximum radiant flux. This is the

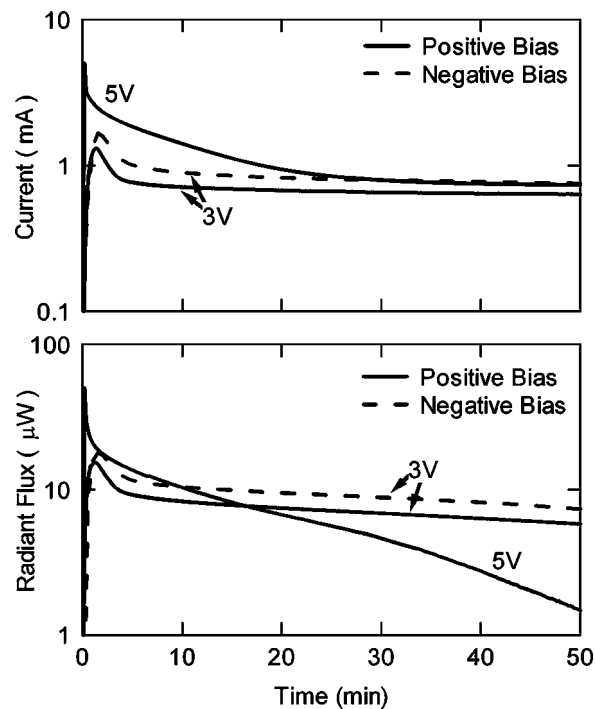


FIG. 1. The current and radiant flux of a standard (single) ITO/ $[\text{Ru}(\text{dtb-bpy})_3]^{2+}(\text{PF}_6^-)_2/\text{Au}$ device operating under +3, -3, and 5 V dc.

time required for ions to redistribute and initiate efficient injection of electrons and holes. At 5 V, the turn-on time is substantially reduced to 0.2 s, but turn-on times on the order of 1–10 ms are needed for 60 Hz operation. Furthermore, this higher voltage leads to a more rapid decay of the radiant flux emitted from the device. Higher voltages lead to even faster turn-on times but also cause rapid device failure due to irreversible degradation of the $[\text{Ru}(\text{dtb-bpy})_3]^{2+}(\text{PF}_6^-)_2$ film.^{3,8} From these observations we see that there are two distinct challenges to overcome in order to fabricate a plug and play device: (1) engineering the material to respond at a 60 Hz frequency and (2) developing a device architecture to withstand the 110–120 V rms amplitude signal supplied by a standard US outlet.

In order to achieve operation at 60 Hz, the turn-on time of the device needs to be improved dramatically. Reducing the thickness of the iTMC layer reduces the turn-on time, but leads to a decrease in the efficiency due to exciton quenching at the electrodes.¹⁷ Increasing the applied bias makes the devices turn on faster, but iTMC-based devices degrade faster at voltages much beyond their turn-on voltage.^{3,8} Pre-biasing schemes³ are not applicable under ac operation. Hence, iTMCs with a high intrinsic ionic conductivity represent the most preferable way to obtain devices with a fast turn-on time. Recently, the ionic liquid $\text{BMIM}^+(\text{PF}_6^-)$ was shown to improve the turn-on time of Ir electroluminescent devices.^{18,19} Incorporation of the $\text{BMIM}^+(\text{PF}_6^-)$ enhanced the ionic conductivity of the device by introducing additional PF_6^- ions into the film and by improving the mobility of the ions in the film. Improvement of the turn-on time of Ir electroluminescent devices by an order of magnitude was demonstrated.

Figure 2 demonstrates light emission upon 60 Hz opera-

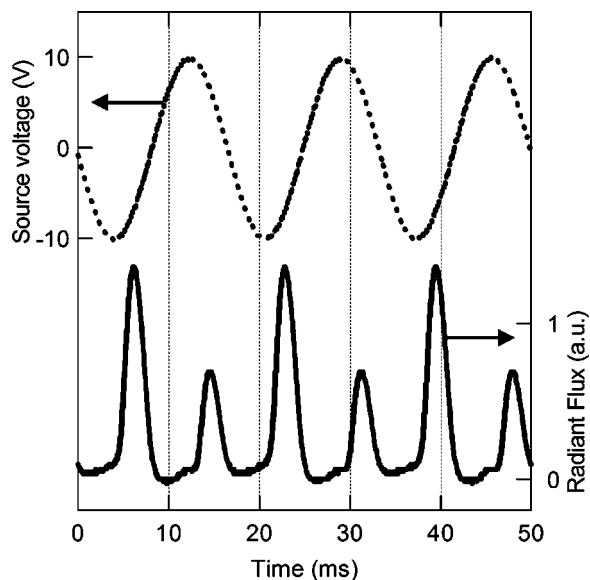


FIG. 2. Source voltage (dotted lines) and radiant flux (solid lines) vs time for a single ITO/[Ru(dtb-bpy)₃]²⁺(PF₆)₂:BMIM⁺(PF₆)⁻/Au device.

tion of a single ITO/[Ru(dtb-bpy)₃]²⁺(PF₆)₂:BMIM⁺(PF₆)⁻/Au device. The dotted line in Fig. 2 shows the source voltage signal—a 60 Hz, 7.1 V rms (20 V peak to peak) ac voltage signal, and the solid line shows the corresponding radiant flux from the device. One can see that light emission occurs following both the positive and negative sweeps of the source voltage, with intervals of no light emission occurring between. The light emission is asymmetric with drive voltage, with a higher emission peak found following the negative voltage sweep from the applied signal. This is consistent with the previous studies^{10,19} of iTMC devices that found ITO to be a better injector of electrons than Au in the transient regime during dc operation. Overall, this radiant flux response corresponds to approximately 3 and 4 μW rms and currents between 300 and 600 μA rms, giving an overall efficiency of 0.25%–0.35%. This is lower than the efficiency previously reported^{8,16} for these devices for operation at 3 V dc. For the present case, two factors contribute to the lower efficiency. First, the device is emitting light for only a fraction of the period of the source signal, as the device is off while the ions redistribute until adequate accumulation/depletion leads to efficient injection of electrons and holes. Secondly, for dc operation it is observed that voltages much beyond the turn-on voltage typically lead to lower efficiencies.^{3,8} For this system, the voltage is sweeping well beyond the dc turn on for a small period of the device operation. It should be noted that at this frequency the device appeared to the eye to be emitting light continuously.

As standard US outlet voltage is 110–120 V rms, it is necessary to implement a device architecture that will withstand high voltages. Recently, Bernards *et al.* used the iTMC [Ru(dtb-bpy)₃]²⁺(PF₆)₂ to demonstrate dc operation of a cascaded device architecture.¹⁶ In this configuration, each electrode acted simultaneously as an anode to one device and as a cathode to its neighbor, as well as an interconnect between the two devices. In this arrangement, for operation of N connected devices, the applied dc voltage was $N \times (3 \text{ V})$. For

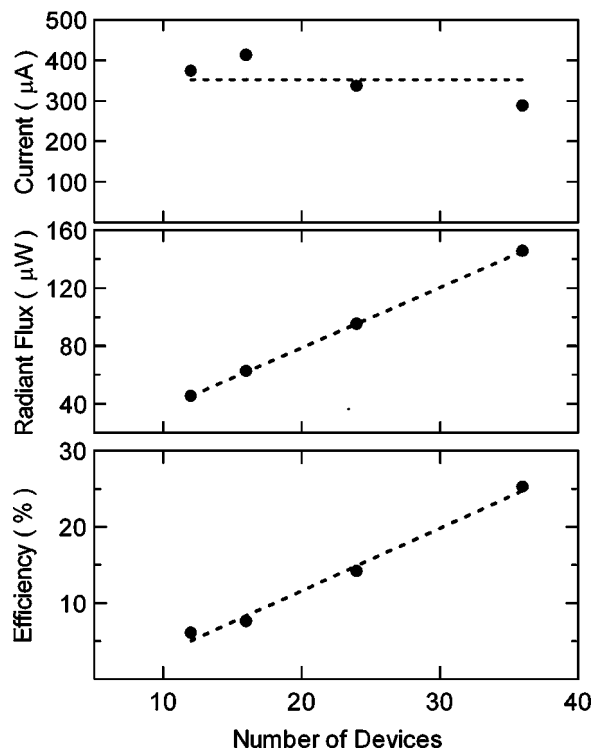


FIG. 3. Current, radiant flux, and external quantum efficiency of a cascaded high voltage test panel operating with $N=12, 16, 24,$ and 36 devices. The dotted lines are guides to the eye.

operation of 1–4 devices, the current of the panel was found to be independent of N , while the radiant flux and external quantum efficiency scaled linearly with voltage. This cascaded architecture provides the added benefit of intrinsic tolerance to electrical shorts.^{16,20,21} Namely, the panel luminance is negligibly affected by the presence of an electrical short. This property makes the cascaded architecture an attractive alternative to a passive matrix architecture and thus a promising technique for the fabrication of large area lighting panels. Furthermore, for appropriate choice of N , this architecture provides a pathway to support the high voltage associated with outlet operation.

For this reason, we constructed the cascaded high voltage test panel. This panel consisted of 96 devices and provided for addressing of variable numbers of cascaded devices, from $N=4$ to 96. We preliminarily operated this architecture at high dc voltages to ensure that the scalability observed for $N \leq 4$ would continue when greater numbers of devices were connected in series. Figure 3 shows the current, radiant flux, and external quantum efficiency of this test panel operating with $N=12, 16, 24,$ and 36 devices at dc applied voltages $V=36, 54, 72,$ and 108 V , respectively. Consistent with the observations for $N \leq 4$, the current remains constant, while the radiant flux and external quantum efficiency clearly scale with N up to the threshold required for outlet operation.

Subsequently, we explored the operation of this high voltage panel directly from a standard US outlet. The rms voltage measured from the outlet was 118 V. Stable operation was observed for $N=16, 24,$ and 36 connected devices. For 16-device operation, the maximum rms external quan-

tum efficiency was 5% at a luminance of 200 cd/m². The half-lives of these panels, the times to decay to 1/2 of the luminance maximum, were approximately 10–20 min. In general, the panel brightness increased and the half-life decreased with decreasing N .

Under 16-device operation, approximately 7.5 V rms is expended per device, which likely contributes to the low half-lives mentioned above. It has been observed for dc voltage operation that device stability is compromised at driving voltage much beyond the turn-on voltage.^{3,8} In addition, these devices were rarely free of electrical shorts, which also contribute to a higher drive voltage per device and shorter lifetimes. When an electrical short develops, due to the symmetry of the architecture, the applied voltage is redistributed across the remaining pixels: 7.5 V rms is dropped across each device in a fully operational 16-device panel operating at 120 V rms, and 8 V rms is dropped across each device in the case of such a panel with one short. While this provides the benefit of increasing the luminance of each device to compensate for the shorted device, this higher voltage also decreases lifetime.

Presumably, reduction of the rms voltage per device would improve stability. One means of reducing this voltage would be to further improve the ionic conductivity in the light emitting layer. This would result in a lower rms voltage per device and involve more devices to drop the full outlet voltage across the panel. The resulting panel would not only be more stable due to the lower rms voltage per device, but would also be more resilient to electrical shorts. For example, if the ionic conductivity could be enhanced to enable sufficiently bright device operation at 4.8 V rms, then 25 devices would be employed to sustain a 120 V rms lighting panel. One electrical short would cause an increase in the device voltage to 5.0 V rms, an incremental change of only 0.2 V rms, as opposed to 0.5 V rms in a 16-device panel. Further improvement in ionic conductivity could make the impact of an electrical short negligible.

This panel can presumably work with other ac signals of different voltage magnitudes by changing the number of devices per panel. For example, accommodation of 220–240 V rms can be achieved by simply doubling the number of connected devices in the panel.

Finally, we demonstrate a cascaded panel in a configuration suitable for lighting purposes (Fig. 4). This panel is comprised of 16 devices each with an active area of 9 mm² with 1 mm separating each device. When fully operational, this gives a lit area of 144 mm² over a total area of 225 mm², or 64% of the total area. This particular panel shown in Fig. 4 has 14 of 16 devices in operation for a total lit area of 56%. The fact that the panel continues to operate with 2 shorted devices demonstrates its inherent fault tolerance to electrical shorts.

IV. CONCLUSIONS

We have demonstrated lighting panels based on ruthenium(II) tris-bipyridine complexes that can be sourced directly from a standard US outlet. With the aid of the ionic liquid 1-butyl-3-methylimidazolium, the conductivity of the

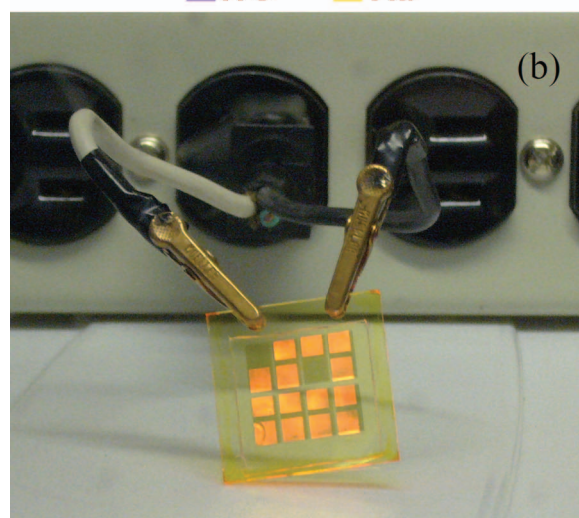
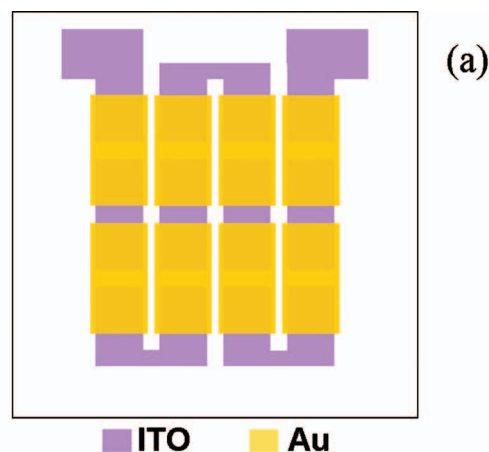


FIG. 4. (Color) (a) Schematic for cascaded lighting panel. (b) Cascaded lighting panel operating directly from a standard outlet.

light emitting layer was enhanced to allow the device to respond at a 60 Hz frequency. The cascaded panel architecture used in this study sustains high input voltages, provides fault tolerance, and facilitates the fabrication of large area solid-state lighting panels. With this architecture, scalability of the drive voltage, radiant flux, and external quantum efficiency is demonstrated for panels with up to $N=36$ devices. Direct outlet operation is achieved for panels with $N=16$, 24, and 36 devices. For a panel with $N=16$ devices, the rms external quantum efficiency is 5% at a luminance of 200 cd/m².

Most significantly, this work reveals that it is possible to fabricate simple light emitting devices that do not require additional circuitry to operate with standard household voltages. Specifically, while conventional LEDs require the use of some dc voltage offset, transformer, and/or ac-to-dc converter to function with a standard US outlet, these iTMC-based cascaded devices work directly from the outlet. The ease of fabrication of these devices provides a cost-effective means of implementing organic light emitting devices for general lighting purposes.

ACKNOWLEDGMENTS

This work was supported by the New York State Office of Science, Technology and Academic Research (NYSTAR)

and by a grant from the Intel Student Research Contest. J.D.S. was supported by a National Science Foundation Graduate Research Fellowship, and D.A.B. was supported by a National Defense Science and Engineering Graduate Fellowship. This work was performed in part at the Cornell NanoScale Facility, a member of the National Nanotechnology Infrastructure Network, which is supported by the National Science Foundation (Grant No. ECS 03-35765).

¹A. Bergh, G. Craford, A. Duggal, and R. Haitz, *Phys. Today* **54**(12), 42 (2001).

²G. G. Malliaras and R. H. Friend, *Phys. Today* **58**(5), 53 (2005).

³E. S. Handy, A. J. Pal, and M. F. Rubner, *J. Am. Chem. Soc.* **121**, 3525 (1999).

⁴F. G. Gao and A. J. Bard, *J. Am. Chem. Soc.* **122**, 7426 (2000).

⁵S. Bernhard, X. Gao, G. G. Malliaras, and H. D. Abruña, *Adv. Mater. (Weinheim, Ger.)* **14**, 433 (2002).

⁶H. Rudmann, S. Shimida, and M. F. Rubner, *J. Am. Chem. Soc.* **124**, 4918 (2002).

⁷M. Buda, G. Kalyuzhny, and A. J. Bard, *J. Am. Chem. Soc.* **124**, 6090 (2002).

⁸S. Bernhard, J. A. Barron, P. L. Houston, H. D. Abruña, J. L. Ruglovksy, X. Gao, and G. G. Malliaras, *J. Am. Chem. Soc.* **124**, 13624 (2002).

⁹J. Slinker, D. Bernards, P. L. Houston, H. D. Abruña, S. Bernhard, and G. G. Malliaras, *Chem. Commun. (Cambridge)* **19**, 2392 (2003).

¹⁰J. D. Slinker, A. A. Gorodetsky, M. S. Lowry, J. Wang, S. Parker, R. Rohl, S. Bernhard, and G. G. Malliaras, *J. Am. Chem. Soc.* **126**, 2763 (2004).

¹¹E. H. Holder, B. M. W. Langeveld, and U. S. Schubert, *Adv. Mater. (Weinheim, Ger.)* **17**, 1109 (2005).

¹²J. C. deMello, N. Tessler, S. C. Graham, and R. H. Friend, *Phys. Rev. B* **57**, 12951 (1998).

¹³J. C. deMello, *Phys. Rev. B* **66**, 235210 (2002).

¹⁴A. A. Gorodetsky, S. Parker, J. D. Slinker, D. A. Bernards, M. H. Wong, G. G. Malliaras, S. Flores-Torres, and H. D. Abruña, *Appl. Phys. Lett.* **84**, 807 (2004).

¹⁵D. A. Bernards, T. Biegala, Z. A. Samuels, J. D. Slinker, G. G. Malliaras, S. Flores-Torres, H. D. Abruña, and J. A. Rogers, *Appl. Phys. Lett.* **84**, 3675 (2004).

¹⁶D. A. Bernards, J. D. Slinker, G. G. Malliaras, S. Flores-Torres, and H. D. Abruña, *Appl. Phys. Lett.* **84**, 4980 (2004).

¹⁷K. W. Lee, J. D. Slinker, A. A. Gorodetsky, S. Flores-Torres, H. D. Abruña, P. L. Houston, and G. G. Malliaras, *Phys. Chem. Chem. Phys.* **5**, 2706 (2003).

¹⁸S. T. Parker, J. D. Slinker, M. S. Lowry, M. P. Cox, S. Bernhard, and G. G. Malliaras, *Chem. Mater.* **17**, 3187 (2005).

¹⁹J. D. Slinker, C. Y. Koh, G. G. Malliaras, M. S. Lowry, and S. Bernhard, *Appl. Phys. Lett.* **86**, 173506 (2005).

²⁰A. R. Duggal, D. F. Foust, W. F. Nealon, and C. M. Heller, *Appl. Phys. Lett.* **82**, 2580 (2003).

²¹J. Kido, T. Matsumoto, T. Nakada, J. Endo, K. Mori, N. Kawamura, and A. Yokoi, *SID Int. Symp. Digest Tech. Papers* **34**, 964 (2003).